FILTERING LENS STRUCTURE BASED ON SRRs IN THE LOW THz BAND

B. Andrés-García and L. E. García-Muñoz

Teoría de la Señal y Comunicaciones
Universidad Carlos III de Madrid
Avenida de la Universidad 30, Madrid 28911, Spain

V. González-Posadas

Ingeniería Audiovisual y Comunicaciones
Universidad Politécnica de Madrid
Carretera de Valencia, Km. 7. Madrid 28031, Spain

F. J. Herraiz-Martínez and D. Segovia-Vargas

Teoría de la Señal y Comunicaciones
Universidad Carlos III de Madrid
Avenida de la Universidad 30, Madrid 28911, Spain

Abstract—A filtering lens for conical horns based on Metamaterials is presented. The paper focuses on a millimeter wave application. The metamaterial structure is composed of a printed layer of Split Ring Resonators (SRRs) on a substrate. The structure is used as a superstrate on the horn aperture. When the SRRs are excited, a filter performance arises preventing radiation in the desired frequency bands. Besides the filtering property, also a lens behavior is achieved. In this way larger gain can be achieved in both E and H planes, reducing the 3 dB beamwidth. A 6% −3 dB stop band is achieved from 73.3 GHz to 85.7 GHz. Symmetrisation of the radiation pattern up to 3 dB is accomplished and the focalization effect is achieved by emulating a hyperbolical-plane lens. Thus, a simplified system based on a conical horn can be designed by unifying the filter and lens in one electromagnetic element.

Corresponding author: B. Andrés-García (belens@tsc.uc3m.es).

1. INTRODUCTION

Research in Quasioptical Systems is focused in the design of lenses or different focalizing elements to transform Quasioptical beams. Usually, typical dielectric lenses for Quasioptical applications are used, introducing losses, that most times are not optimal either acceptable designs for applications such as Radioastronomy [1], Security and Medicine.

Conical horns are wideband elements, making sometimes necessary the design of filters to suppress the non-desired frequencies. Filters in the submillimeter frequencies based on waveguide technology present high complexity, costing and manufacturing problems. Replacing a waveguide filter with a system designed in planar technology allows miniaturization and reduction of complexity and cost of the entire scheme.

During the last years many researches are focused on metamaterials and their filtering properties designed for their application inside waveguides [2], antennas [3–6] and circuits [7]. Some of them present good results in the low Terahertz band (from 70 GHz to 100 GHz) [8, 9] as the current paper. In addition to the filtering performance, metamaterials present lenses properties [10]. Finally, metamaterial properties combined in a periodic structure presents Frequency Selective Surfaces (FSS) performance [11, 16].

The metamaterial particle used in this paper is the square SRR. The designed structure is placed as a superstrate for the conical horn [10, 12] presenting filtering and lens behaviour. It shows a stop band filter performance, which suppresses the non-desired frequencies. The filter electromagnetic behaviour can be controlled with the geometric parameters of the proposed structure. In addition, the non symmetric E- and H-plane radiation patterns of the conical horn can also be symmetrised by the presence of the metamaterials layer. The conical horn used in this paper is working at the millimeter band. The simulations have been carried out with the horn excited in the fundamental mode TE_{11} from 60 GHz to 100 GHz.

The lens effect achieved with this structure allows planar technology [15, 17]. This structure emulates a hyperbolic-plane lens, making easier the manufacturing process than for conventional lenses, which are difficult to design and manufacture due to their conical shape.

The paper is organized as follows: First of all, the isolated SRR is studied, continuing with the composite structure. In Section 2, a single layer structure is presented. For this task, the designed structure is first presented. Once the properties of the structure are known, simulations

with a dielectric sheet are presented. In Section 3, the structure is replicated in a way that a two-layer structure is proposed. When the behaviour of the system without dielectric is known, Teflon is placed between the two layers to improve the specifications of the filter.

2. STRUCTURE WITH ONE METAMATERIAL LAYER

2.1. Structure without Dielectric

The designed structure is shown in Fig. 1. The operation frequency band goes from 60 GHz to 100 GHz, with the horn excited in the fundamental mode TE_{11}. Simulations have been carried out with CST Microwave Studio 2008.

The stop-band filter is placed at the centre of the band. The proposed structure is composed of SRRs in a periodic-planar configuration and it is placed at the horn aperture. All the lengths are given in terms of the wavelength, taking λ_0 at 80 GHz, which is 3.75 mm.

The specifications for a single SRR and for the composite structure are detailed in Table 1, and in Fig. 2.

With all these parameters the resonant frequency for one isolated SRR is 96.9 GHz. This result has been tested by placing an isolated SRR into a rectangular waveguide as shown by [2, 13]. The filter electromagnetic behaviour can be controlled with the geometric parameters of the proposed structure. The required resonant frequency is mainly tuneable with the IL parameter and with d, c, and e for a fine adjustment. The inter-element spacing is set slightly below $\lambda/4$ at the central frequency or the filter (82 GHz). For larger spacing
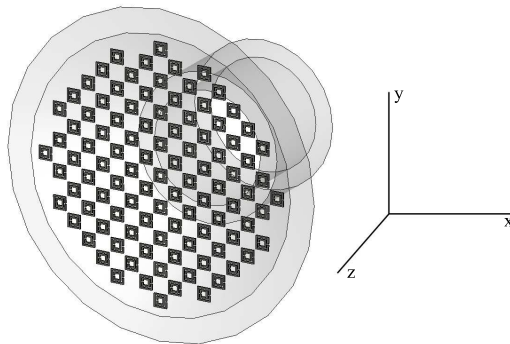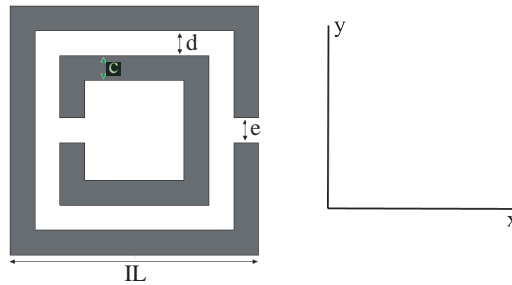

Figure 1. Horn antenna with the planar metamaterial structure proposed in the mouth.

Table 1. Specifications for the structure (normalized to λ_0).

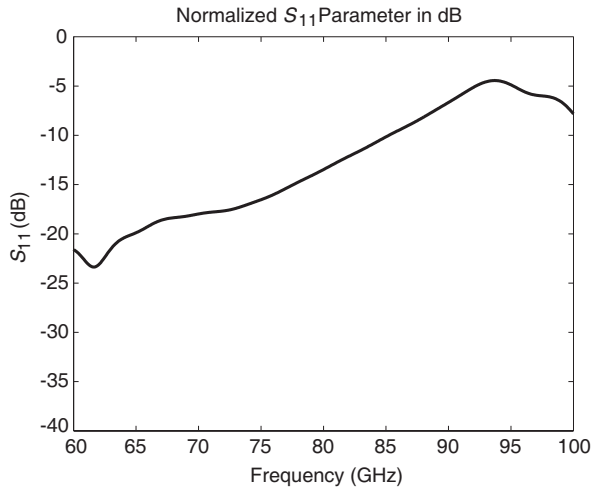| Parameter	Value
IL	0.1013
d	0.0101
c	0.0101
e	0.0101
Inter-element spacing	0.232

Figure 2. Geommetry of the SRR.

between elements, the periodic structure is not excited, so the filtering behavior is not present. Moreover, the filter is more selective and the lens performance is strengthened when the inter-element spacing gets as close as possible to the limit $\lambda/4$, but without reaching it. In Section 3 will be specified all the variations for these parameters and tolerance studies for the final designed system.

The simulated S_{11} parameter is shown in Fig. 3(a). A filtering effect is observed at the SRRs resonant frequency, but the rejection level in the stop band is not enough either the bandwidth is not well defined. These specifications are not acceptable for the filter requirements.
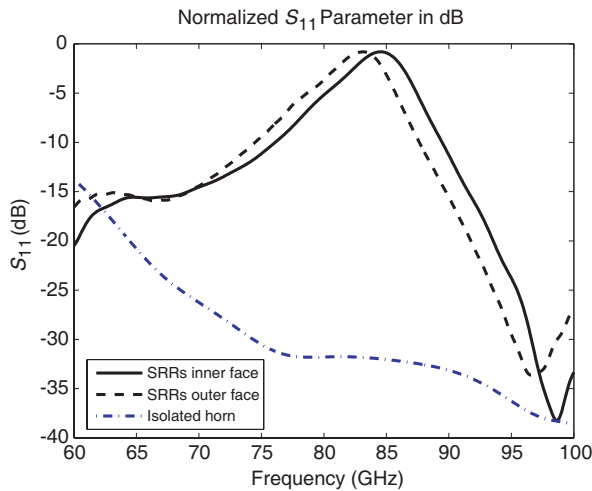
2.2. Structure with Dielectric

In order to achieve a well-defined stop-band, the SRRs are printed on a dielectric sheet. Also it makes practical manufacturing possible. The dielectric substrate is Teflon, with ϵ_r of 2.08, and a width of 0.1 mm ($0.027\lambda_0$). The lowest possible thickness for the substrate has been chosen to reduce the losses in the pass-bands.

There are two possible ways for setting up the structure: The SRRs can be printed in the inner or in the outer face of the dielectric. The structure is placed at the horn aperture for the SRRs printed in the inner face of the dielectric and at $0.027\lambda_0$ outside the horn aperture for the SRRs printed in the outer face. The results of both simulations are presented in Fig. 3(b).

Normalized S_{11} Parameter in dB

(a) Structure without dielectric

Normalized S_{11} Parameter in dB

(b) Structure printed on Teflon

Figure 3. S_{11} parameter for the one-layer structure.

The rejection level has been increased by 3.4 dB in the stop-band region with respect to the case without dielectric. In comparison with the air simulation, the resonant frequency has been shifted down to 83.1 GHz (14.2%) for the SRRs printed in the outer face, and to 84.6 GHz (12.7%) for the inner case due to the change in the effective dielectric permittivity. For the inner and outer case bandwidth and rejection level are the same.

An important issue for this structure is the polarization angle of the electric field. In Fig. 4, the S_{11} parameter is shown for several polarization angles. The maximum excitation of the SRRs is achieved for vertical polarization (Y-axis, 90°). According to [2], in this case the electric field is the responsible of the excitation of the SRRs. As shown in Fig. 4, when the polarization becomes horizontal (X-axis, 0°), the filtering effect disappears. Despite of this, the structure does not cause any alteration in the linear polarization of the radiated field.

These simulations correspond to the SRRs printed on the inner face of the dielectric, nevertheless, equal effects are observed when the SRRs are printed on the other side.

According to our simulations, if the structure is placed inside the horn in the $-Z$ direction, the bandwidth and the central frequency of the filter are not modified or shifted. However, the rejection level in the stop-band decreases because of not only the SRRs number decreases but also because they are excited in a poorer way.
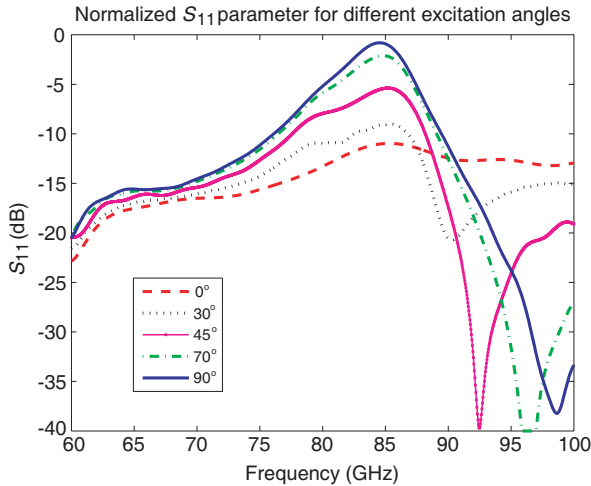

Figure 4. S_{11} parameter for the one-layer structure for different polarization angles.

Regarding the radiation patterns for this system, two behaviors should be considered: Y- and X-polarization. The radiation patterns are shown in Figs. 5 and 6 for the SRRs printed in the inner face of the dielectric. The radiation patterns for the outer face case are not plotted here as they have no significant variations. However, the -3 dB beamwidths and gain paramters are shown later. The radiation patterns correspond to both polarizations and for the upper (100 GHz) and the lower band (65 GHz).

(a) 65 GHz E-plane (b) 65 GHz H-plane

(c) 100 GHz E-plane (d) 100 GHz H-plane

Figure 5. Radiation patterns for the SRRs printed in the inner face of the dielectric for polarization on the Y-axis (solid) in comparison with the isolated horn (dashed).

(a) 65 GHz *E*-plane

(b) 65 GHz *H*-plane

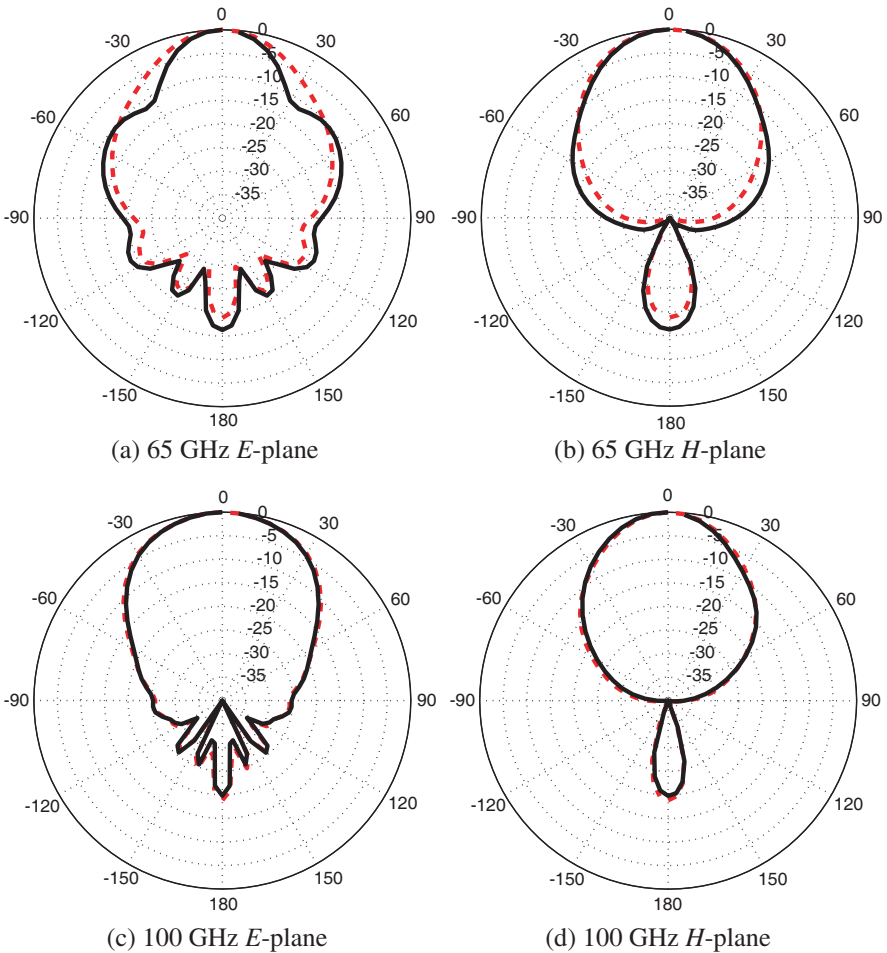(c) 100 GHz *E*-plane

(d) 100 GHz *H*-plane

Figure 6. Radiation patterns for the SRRs printed in the inner face of the dielectric for polarization on the *X*-axis (solid) in comparison with the isolated horn (dashed).
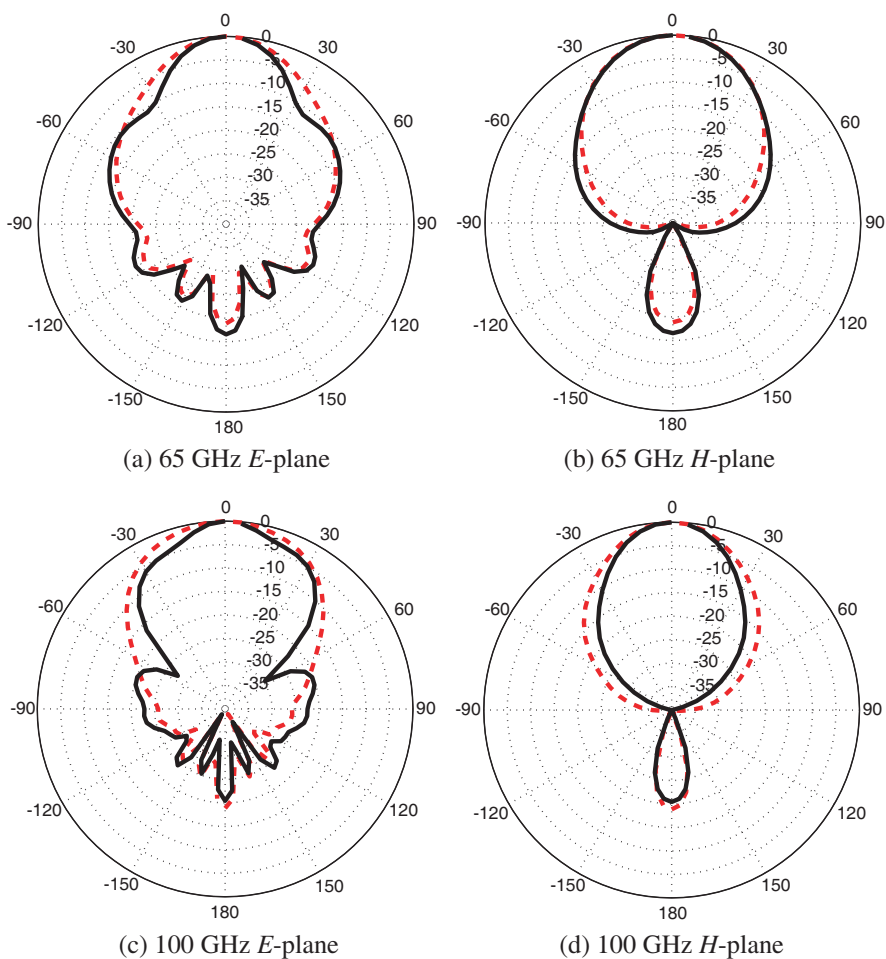
Table 2. 3 dB beamwidths for the isolated horn.

Frequency	*E*-Plane	*H*-Plane
65 GHz	37.9°	41.3°
100 GHz	51.5°	34.0°

Table 3. $3\,$dB beamwidths for horn+structure for polarization along Y-axis.

Frequency	E-Plane (inner)	H-Plane (inner)	E-Plane (outer)	H-Plane (outer)
65 GHz	29.2°	38.0°	28.3°	38.3°
100 GHz	50.2°	34.1°	49.5°	34.3°

Table 4. $3\,$dB beamwidths for horn+structure for polarization along X-axis.

Frequency	E-Plane (inner)	H-Plane (inner)	E-Plane (outer)	H-Plane (outer)
65 GHz	30.4°	40.0°	30.0°	40.5°
100 GHz	31.6°	29.6°	32.1(53)°	26.7°

For the SRRs printed in the inner face of the dielectric, and when the filtering behavior is achieved (Y-polarization, $90°$), the radiation patterns remain equal as for the isolated horn, specially for the high-band. At the low band there is a slight difference in the E-plane. The $-3\,$dB beamwidth becomes $8.7°$ narrower and a side-lobe level appears, with a normalized level of $-10.4\,$dB. When no filtering behavior is achieved (X-polarization, $0°$), stronger lens effect is observed. As shown in Fig. 6 and in Table 4, both E- and H-plane beamwidths are reduced by $18.1°$ and $4.4°$ at $100\,$GHz. At this frequency, a strong symmetrization at $-3\,$dB of the beam is accomplished. While in the original horn the difference between beamwidths for both planes is $17.5°$, for the proposed structure is $2°$. For the low band, the structure presents the same behaviour as for the other polarization.

Regarding the case of the SRRs printed in the outer face of the dielectric, equal effects are observed, as can be seen in Table 3 and Table 4. For the case of horizontal polarization the side-lobe level in the E-plane is $-8.8\,$dB, so it is slightly higher than for vertical polarization.

All the parameters for these plots are shown in Tables from 2 to 4, including the parameters for the original horn. As reported by [11], both structures are not reciprocal, and the structure for the SRRs printed on the inner face has a better performance, with a lower level of side-lobes.

Along the stop-band region, a distortion of the beam is achieved, because the far-field plot is slightly distorted when the SRRs are excited in both the E- and H-plane.

The gains for this system are specified from Tables 5 to 7. It is remarkable the increase in gain for the structure when no filtering behaviour is foreseen.

Table 5. Gain for the isolated horn in dB.

Frequency	Original Horn
65 GHz	12.6
100 GHz	12.7

Table 6. Gain in dB for horn+structure for polarization along the Y-axis.

Frequency	Inner face	Outer face
65 GHz	13	12.3
100 GHz	12.9	12.9

Table 7. Gain in dB for horn+structure for polarization along the X-axis.

Frequency	Inner face	Outer face
65 GHz	12.9	12.5
100 GHz	14.5	13.6

With all these results gathered together, should be concluded that a single layer of SRRs achieves a stop band region for the conical horn. Despite of this, the needed for a more selective filter arises. Lens effect is accomplished for certain polarizations specially at the high band. It is important to remark also the symetrization of the beam achieved.

3. STRUCTURE WITH TWO METAMATERIAL LAYERS

The objective for this section is to achive the highest rejecting level in the stop band, while in the pass band region the losses should remain below -10 dB. In addition, a more selective filter is desired. First of all, a second layer of SRRs is placed in the horn aperture, without dielectric. Secondly, a planar dielectric sheet is placed with the SRRs printed on both sides.

3.1. Structure without Dielectric

According to the previous results, the need of a more selective filter arises. This is achieved by placing a second layer of SRRs in the aperture of the horn. This second layer must be slightly scaled with respect to the previous one, so that the SRRs resonate at a close frequency. The objective is to increase the bandwidth based on

modifying the size of the SRRs [14]. For this case, the SRRs are scaled 98% with respect to the first layer in both X and Y planes. The same size for each SRR as in Section 2 is employed for the inner layer. With these parameters, the resonant frequency for the inner layer remains at 96.9 GHz while the frequency for the SRRs on the second layer is 98.6 GHz.

The spacing between elements remains constant in both layers, as explained in Section 2. The restriction of $\lambda/4$ (at the central frequency of the filter, 82 GHz) is also applicable to the current case. The spacing between each layer should be as small as possible for the sake of practical manufacturing. This is done because if the distance between layers increases, the filtering effect disappears. For manufacturing purposes and a good trade-off for the spacing has been set to 0.1 mm $(0.027\lambda_0)$.

Table 8. Parameters for the two-layer filter (Frequencies in GHz).

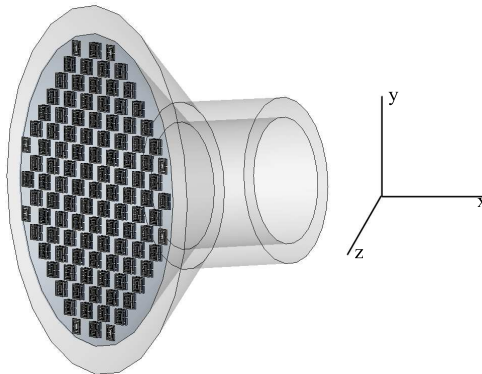|	
3 dB Bandwidth	3.8%
10 dB Bandwidth	17.7%
Fpass1	78.6
Fstop1	88.1
Fstop2	91.5
Fpass2	94.5
Central Frequency	90
Maximum rejection level	−2.5 dB

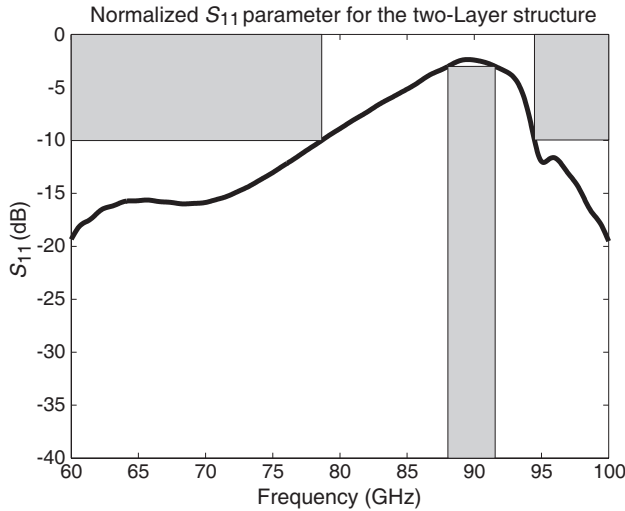**Figure 7.** Horn with the two-layer periodic structure.

Figure 8. S_{11} parameter for the two-layer structure.

The simulated structure is shown in Fig. 7 and the S_{11} parameter is shown in Fig. 8. The achieved filter is more selective than the one-layer structure, and achieves higher rejection levels in the stop-band for the same case than the one without dielectric. The reflection coefficient for the central frequency corresponds to a normalized S_{11} level of $-2.5\,\mathrm{dB}$. The specifications for this filter are shown in Table 8. The transition band for this S_{11} is slow. The next section presents the methodology for increasing the slope of that curve.

3.2. Structure Filled with Dielectric

According to the previous results, it is desired to achieve a higher rejection level in the stop band. Also, it is desired to reduce the band between $-3\,\mathrm{dB}$ and $-10\,\mathrm{dB}$, thus, a more selective filter could be obtained. Teflon is used as substrate for printing the SRRs, as done in Section 2. This material is well known for its use in Quasioptical systems for the construction of lenses and it is almost transparent to these frequencies [1].

The result of placing the dielectric between both layers is shown in Fig. 9. The change of the dielectric constant causes a shift on the peak in the S_{11} towards lower frequencies of $8.5\,\mathrm{GHz}$ (10.4%) with respect to the structure without dielectric. Regarding the rejection level within this band, the maximum value of the S_{11} parameter is $-0.9\,\mathrm{dB}$, so it is increased by $1.6\,\mathrm{dB}$. The parameters for the final result of this filter
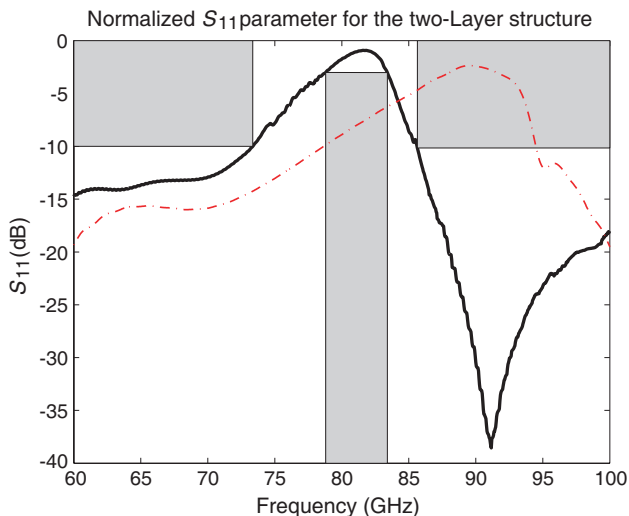
Figure 9. S_{11} parameter for the structure filled with Teflon (solid) in comparison with the structure without Teflon (dashed).

Table 9. Parameters for the two-layer filter filled with Teflon (Frequencies in GHz).

3 dB Bandwidth	6%
10 dB Bandwidth	12.7%
Fpass1	73.4
Fstop1	78.7
Fstop2	83.6
Fpass2	85.5
Central Frequency	81.7
Maximum rejection level	−0.9 dB

are shown in Table 9. The bandwidth between the levels −10 dB and −3 dB on the low band has been reduced from 9.5 GHz to 5.3 GHz. A −3 dB bandwidth of 6% has been achieved with this structure in comparison with the previous 3% bandwidth of the one layer case.

The simulations of the S_{11} parameter are shown in Fig. 10 versus three field polarization angles. The polarization of 90° corresponds to an E-field along the Y-axis, where the SRR is mostly excited. The polarization of 0° corresponds to an E-field along X-axis, where the filter is not excited.

For comparison purposes a Butterworth filter is designed with equal specifications. For achieving an asymmetrical response, a 32th order filter is needed, with 14 stages. The Butterworth mask for this filter is shown in Fig. 11.
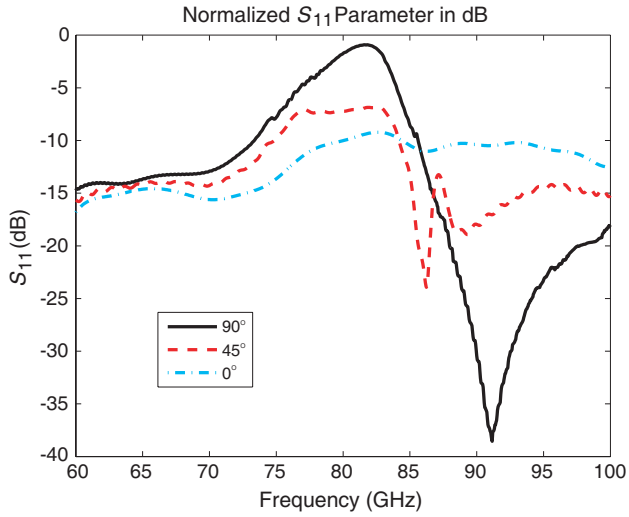

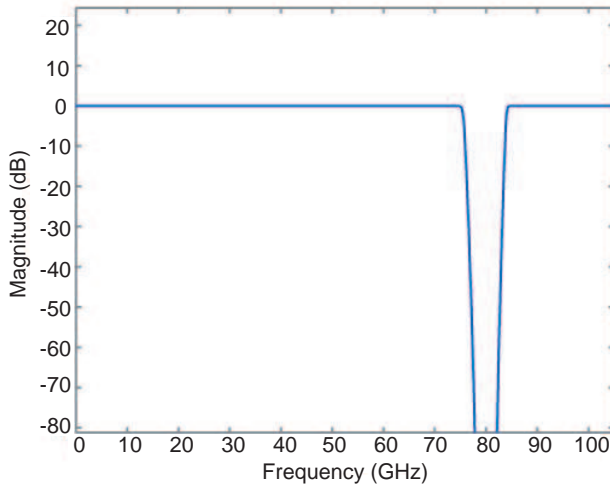**Figure 10.** Normalized S_{11} parameter for different polarization angles.

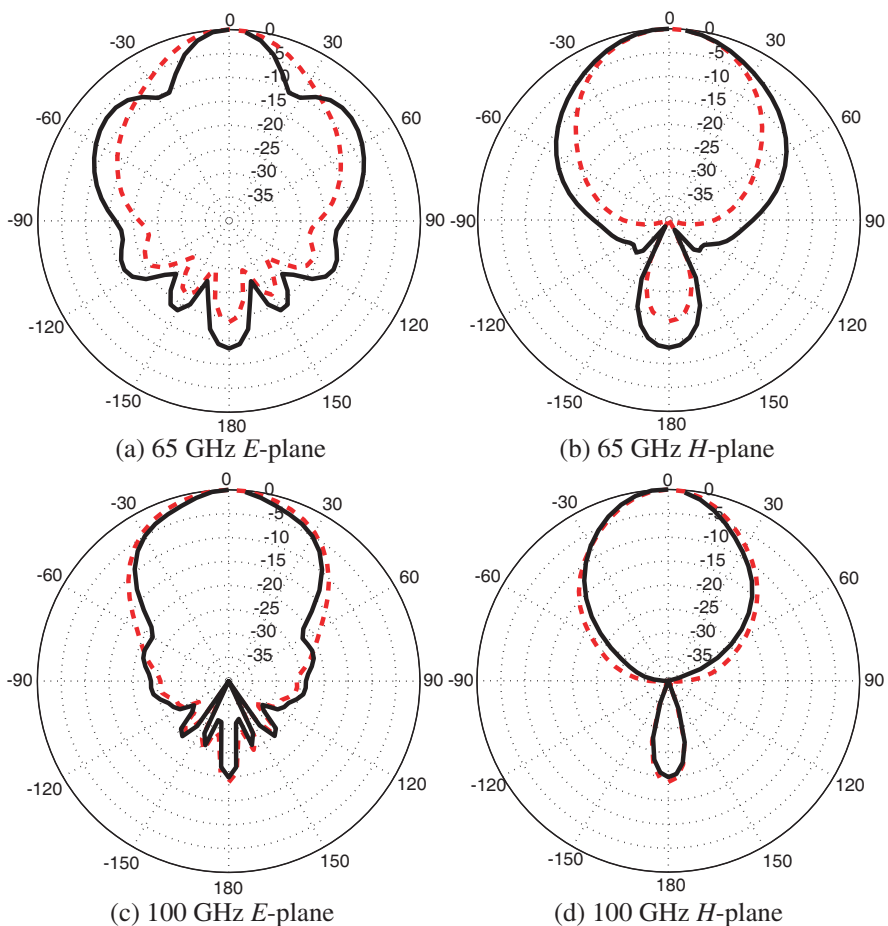**Figure 11.** Butterworth equivalent filter.

Figure 12. Radiation patterns for polarization along the Y-axis. Isolated horn (dashed) and horn plus lens (solid).

Regarding the radiation patterns, the same effects as in Section 2 are observed depending on the polarization angle. A stronger lens effect is achieved when the electric field is polarized along the X direction in the higher band, when there is no filtering effect (Fig. 13). The strongest effect is achieved for the H-plane where a reduction of $10.9°$ of the beamwidth is accomplished at 100 GHz. For 65 GHz, the reduction in the E-plane remains constant as in the one-layer case, while for the H-plane the main beam is slightly broadened. For polarization along the X-axis the same effect is observed. For this case, the difference in beamwidths is $7.4°$ while in the original horn is $17.5°$. Thus, the symmetrizing effect is achieved for both polarizations while a lens effect

is accomplished for polarization along X-axis.

Figure 12 shows the results for polarization along the Y-axis. The structure produces a symmetrization of the beam: While the difference between the E- and H-plane is $17.5°$ for the isolated horn, with the structure, the difference is reduced to $8.2°$. In the stop-band and transition regions, a distortion of the radiation pattern appears, as presented in Fig. 14. In this way, not only a high isolation level is achieved with the S_{11}, but the distorted radiation pattern in the main direction allows the introduction of a minimum.
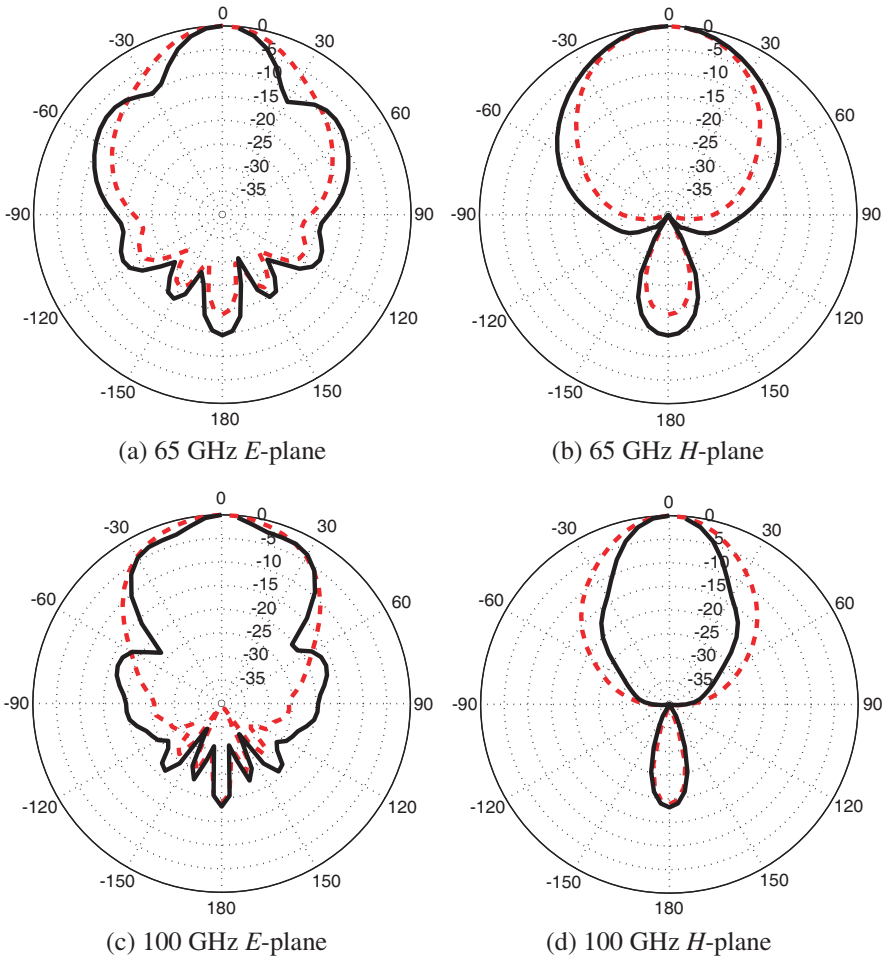

(a) 65 GHz E-plane

(b) 65 GHz H-plane

(c) 100 GHz E-plane

(d) 100 GHz H-plane

Figure 13. Radiation patterns for polarization along the X-axis. Isolated horn (dashed) and horn plus structure (solid).

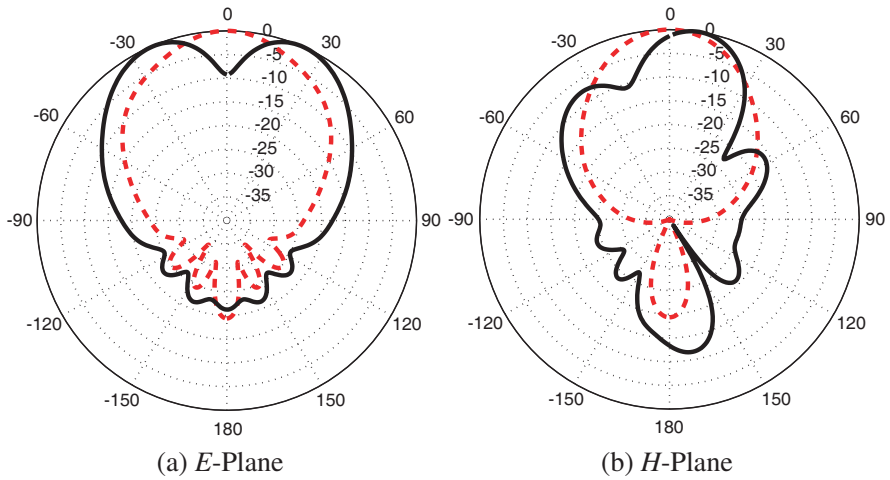(a) *E*-Plane   (b) *H*-Plane

Figure 14. Radiation pattern for 81.7 GHz. Isolated horn (dashed) and horn plus lens (solid).

Table 10. 3 dB beamwidths for the two-layer structure and polarization along the *Y*-axis.

Frequency	*E*-Plane	*H*-Plane	*E*-Plane (isolated)	*H*-Plane (isolated)
65 GHz	25.5°	46.0°	37.9°	41.3°
100 GHz	41.2°	33.0°	51.5°	34.0°

Table 11. 3 dB beamwidths for the two-layer structure and polarization along the *X*-axis.

Frequency	*E*-Plane	*H*-Plane	*E*-Plane (isolated)	*H*-Plane (isolated)
65 GHz	27.0°	46.7°	37.9°	41.3°
100 GHz	32.1°	24.7°	51.5°	34.0°

Table 12. Gain in dB for the two-layer structure.

Frequency	Isolated Horn	Horn+Structure (Vertical)	Horn+Structure (Horizontal)
65 GHz	12.6	10.8	11.7
100 GHz	12.7	13.5	14.3

Both the E- and H-plane are symmetric within the -3 dB beamwidth and the -5 dB point is placed for both planes at ($50°$) at 100 GHz.

The gain for the final system is always increased except for the case when the filter is excited in the low band. These specifications are shown in Table 12. It must be pointed out that an increase of 1.6 dB in the high band when the structure shows lens properties.

3.3. Tolerance Studies

In this section, the tolerance studies are presented. As the metamaterials are resonating structures, they present a high quality factor which produces a low tolerance in manufacturing. First of all, the parameters analysis tolerance for the SRR are presented following with the discussion of the results with the variation of the parameters for the periodic structure in the horn aperture.

The variations of the parameters such as c, d and e, for the SRRs are not critical. Simulations with a variation of $\pm 10\%$ (4 μm) for c and d show a frequency shift of ± 1.5 GHz (1.8%) in the central frequency of the filter. The bandwidth remains constant. This implies that these parameters can be used for a fine adjustment of the central frequency. Regarding the e parameter, the shift in frequency can be ignored, as it produces minor variations in the S_{11} parameter.

Concerning the size of the SRR, the parameter IL is extremely critical. A variation of $\pm 2.5\%$ (± 10 μm) induce a frequency shift of 4 GHz (5%) for the central frequency, so the filter could be tunable between a wide range of frequencies.

Regarding the parameters of the periodic structure, simulations of the distance between elements have been done. As the distance between SRRs decreases, the periodicity of the structure also decreases, increasing the S_{11} parameter up to the -10 dB level. A decrease of an 8% in this distance, produces losses in the lower band of -8.8 dB. On the other hand, if this parameter is increased a resonance in the stopband arises when the limit of $\lambda/4$ (6.4%) and the filtering effect is not achieved, thus it is also a critical parameter.

Regarding the distance between layers, as it increases, the level of rejection in the whole band is also increased. When it is doubled, i.e., increased to $0.0534\lambda_0$ the band is also increased to 20% at a level of -10 dB, and the losses in the low band are -10 dB. Thus the specifications for the filter are not accomplished. The reduction of this distance can not be considered due to manufacturing processes.

4. CONCLUSIONS

A structure with filtering and lens performance has been developed. This filter operates in the band of 60–100 GHz, with 6% bandwidth at −3 dB. This is achieved with the excitation of a periodic structure based on SRRs. The lens performance is specially achieved for the high band, having a symmetrization of the beam at −3 dB.

REFERENCES

1. Goldsmith, P. F., *Quasioptical Systems*, IEEE Press/Champman & Hall Publishers Series on Microwave Technology and RF, 1997.

2. Marques, R., F. Martin, and M. Sorolla, *Metamaterials with Negative Parameters*, Wiley Series in Microwave and Optical Engineering, 2008.

3. Herraiz, F. J., L. E. García-Muñoz, V. González-Posadas, and D. Segovia-Vargas, "Multi-frequency and dual mode patch antennas partially filled with left-handed structures," *IEEE Transactions on Antennas and Propagation*, Vol. 58, No. 8, Part 2, 2527–2539, 2008.

4. Herraiz-Martínez, F. J., E. Ugarte-Muñoz, V. González-Posadas, L. E. García-Muñoz, and D. Segovia-Vargas, "Self-diplexed patch antennas based on metamaterials for RFID Active systems," *IEEE Transactions on Microwave Theory and Techniques*, Special Issue on RFID, accepted for publication.

5. Yu, A., F. Yang, and A. Elsherbeni, "A dual band circularly polarized ring antenna based on composite right and left handed metamaterials," *Progress In Electromagnetics Research*, PIER 78, No. 73–81, 2008.

6. Si, L. M. and X. Lv, "CPW-fed multi-band omni-directional planar microstrip antenna using composite metamaterial resonators for wireless communications," *Progress In Electromagnetics Research*, PIER 83, No. 133–146, 2008.

7. Castro-Galán, D., L. E. García-Muñoz, D. Segovia-Vargas, and V. González-Posadas, "Diversity monopulse antenna based on a dual-frequency and dual mode clrh rat-race coupler," *Progress In Electromagnetics Research B*, Vol. 8, 87–106, 2009.

8. Chen, H. T., W. J. Padilla, R. D. Averitt, A. C. Gossard, C. Highstrete, M. Lee, J. F. O'Hara, and A. J. Taylor, "Electromagnetic metamaterials for terahertz applications," *Terahertz Science and Technology*, Vol. 1, No. 1, March 2008.

9. Duan, Z. Y., B. I. Wu, S. Xi, H. S. Chen, and M. Chen,

"Research progress in reversed cherenkov radiation in double-negative metamaterials," *Progress In Electromagnetics Research*, PIER 90, No. 75–87, 2009.

10. Liu, Y. H. and X. P. Zhao, "Investigation of anisotropic negative permeability medium cover for patch antenna," *IET Microw. Antennas Propag.*, Vol. 2, No. 7, 737–744, 2008.

11. Munk, B. A., *Frequency Selective Surfaces*, John Wiley & Sons, 2000.

12. Huang, M. D. and S. Y. Tan, "Efficient electrically small prolate spheroidal antennas coated with a shell of double-netagive metamaterials," *Progress In Electromagnetics Research*, PIER 82, No. 241–255, 2008.

13. Caloz, C. and T. Itoh, *Electromagnetic Metamaterials. Transmission Line Theory and Microwave Applications*, John Wiley & Sons, 2006.

14. Herraiz, F. J., L. E. García-Muñoz, V. González-Posadas, D. Segovia-Vargas, D. González-Ovejero, and C. Craeye, "Arrays of dual-band printed dipoles loaded with metamaterial particles," *Third European Conference on Antennas and Propagation*, Berlin, March 2009.

15. Wu, B. I. and J. A. Kong, "Experimental confirmation of guidance properties using planar anisotropic left-handed metamaterial slabs based on S-ring resonators," *Progress In Electromagnetics Research*, PIER 84, No. 279–287, 2008.

16. Liu, S. H., C. H. Liang, W. Ding, L. Chen, and W. T. Pan, "Electromagnetic wave propagation through a slab waveguide of uniaxially anisotropic dispersive metamaterial," *Progress In Electromagnetics Research*, PIER 76, No. 467–475, 2007.

17. Naqvi, Q. A., "Planar slab of chiral nihility metamaterial backed by fractional dual/PEMC interface," *Progress In Electromagnetics Research*, PIER 85, No. 381–391, 2008.